Special Issue

Statistic Replacement of Lanthanide Ions in Bis-salicylatoborate Coordination Polymers for the Deliberate Control of the Luminescence Chromaticity

Sven H. Zottnick,[b] Jan A. P. Sprenger,[b, c] Maik Finze,[b, c] and Klaus Müller-Buschbaum*[a, b, d]

Based on the strand-like coordination polymer (CP) type $^1_\infty$[Ln(BSB)$_3$(py)$_2$], [BSB]$^-$ = bis-salicylatoborate anion, mixed Eu/Tb-containing compounds of the constitution $^1_\infty$[Eu$_x$Tb$_{1-x}$(BSB)$_3$(py)$_2$] were synthesised ionothermally for a phase width of (x = 0.25–0.75) and characterized regarding structure and optical properties. Previously, known only for other lanthanides, the mixed 1D–Eu/Tb-CPs show excellent options for statistic replacement of the Ln-cations during synthesis yielding solid solutions. The products are highly luminescent, with the chromaticity being a direct function of the amount of the respective Ln-ions. Corresponding to an overall addition of emission intensities, the green Tb^{3+} emission and the red Eu^{3+} emission allow for a chromaticity control that also includes yellow emission. Control of the luminescence colour renders them suitable examples of the versatility of statistic replacement of metal ions in coordination chemistry. In addition, crystallization of [EMIm]$_2$[YCl$_5$(py)] illuminates possible other products of the ionothermal reactions of [EMIm][BSB] with LnCl$_3$ constituted by components not being part of the main CPs.

1. Introduction

Luminescent coordination polymers (CPs) and metal-organic frameworks (MOFs) have attracted wide attention in recent years, as they provide a wide variety of options to influence the luminescence processes by selection of ligands and metal centers up to remarkable options for chemical and physical sensing.[1]

Spiroborates can be utilized for the synthesis of new complexes, coordination polymers (CPs), covalent organic frameworks (COFs), and supramolecular polymers.[2] As they exhibit functional groups, they can act as potential linkers suitable for multiple coordination to metal ions. Currently, organic oxoborates are investigated for potential applications in semi-conductors[3] or as electrolytes in Li-ion batteries,[4–7] Remarkably, they are also known as anions in ionic liquids and low-melting salts.[8] Still, mainly salts with alkaline metal or organic cations are known,[9] while the knowledge on the coordination of such spiroborate anions, e.g. for lanthanide coordination compounds, is limited. Investigations on the reactivity of different oxalatoborates, such as [EMIm][Catbox] or Li[BOB] (EMIm = 1-ethyl-3-methyl-imidazolium) in the presence of lanthanide chlorides or nitrates even showed decomposition of the respective borate anion rather than a coordination to the lanthanide ions.[10] A few examples of Ln-compounds are known of the anions tetra(methoxy)borate or catecholatoborate, namely [Ln{B(OCH$_3$)$_4$}(NO$_3$)$_2$(CH$_3$OH)$_2$] (Ln=La, Pr, Nd)[11] and [{Na}{(sal)$_3$Ln(B(OCH$_3$)$_4$)Ln(sal)$_3$}]$_n$ (sal = salicylato and Ln=Y, Nd, Eu–Lu)[12] and [(η^2-catecholato-μ-catecholatoborate)$_3$Ln(thf)$_3$]·thf (Ln=Nd, Sm).[13] In this context, we could also show that the low-melting salt [EMIm][BPB] ([BPB]$^-$ = bis(phthalato)borate anion; [B{(C$_6$H$_4$)(CO$_2$CO$_2$)}$_2$]$^-$) could be transformed into a coordination polymer together with Tb^{3+}, $^1_\infty$[Tb(o-HBDC)(H$_2$O)$_6$][BPB]$_2$.[14]

Amongst the different spiroborates, the bis-salicylatoborate anion [BSB]$^-$ proofed to be a useful anion together with lanthanides due to the intense luminescence of the products, with the anion [BSB]$^-$ being a versatile sensitizer for the lanthanide luminescence. Thus, the [BSB]$^-$ is among the ligands that allow an efficient transfer of energy from the respective ligand onto the lanthanide ions, which is vital for a successful sensitization of the otherwise low light uptake of trivalent

[a] Prof. Dr. K. Müller-Buschbaum
Institut für Anorganische und Analytische Chemie
Justus-Liebig Universität Gießen
Heinrich-Buff-Ring 17
35392 Gießen (Germany)
E-mail: kmbac@uni-giessen.de
[b] Dr. S. H. Zottnick, Dr. J. A. P. Sprenger, Prof. Dr. M. Finze, Prof. Dr. K. Müller-Buschbaum
Institut für Anorganische Chemie
Julius-Maximilians-Universität Würzburg
Am Hubland
97074 Würzburg (Germany)
[c] Dr. J. A. P. Sprenger, Prof. Dr. M. Finze
Institut für nachhaltige Chemie & Katalyse mit Bor (ICB)
Julius-Maximilians-Universität Würzburg
Am Hubland
97074 Würzburg (Germany)
[d] Prof. Dr. K. Müller-Buschbaum
Center for Materials Research (LAMA)
Justus-Liebig University Gießen
Heinrich-Buff-Ring 16
35392 Gießen (Germany)

Supporting information for this article is available on the WWW under https://doi.org/10.1002/open.202000251

Special Issue

An invited contribution to a Special Issue dedicated to Material Synthesis in Ionic Liquids

© 2021 The Authors. Published by Wiley-VCH GmbH. This is an open access article under the terms of the Creative Commons Attribution Non-Commercial NoDerivs License, which permits use and distribution in any medium, provided the original work is properly cited, the use is non-commercial and no modifications or adaptations are made.

lanthanide ions due to the parity forbidden character of the 4f-transitions.[15] Together with the $[BSB]^-$ anion, one- and two-dimensional coordination polymers and networks of the constituents were reported, recently: $^1_\infty[Ln(BSB)_3(py)_2]$ (Ln=Y, La–Nd, Sm)[16] and $^2_\infty[Ln(BSB)_3(py)]$ (Ln=Sm, Eu, Tb, Dy, Er).[16b]

Herein, we present further examples for one-dimensional coordination polymers expanding Ln to mixtures of Eu^{3+} and Tb^{3+}, and elaborate on the intense photoluminescence that can be utilized for a deliberate control of the luminescence chromaticity between green and red by statistic replacement of the trivalent lanthanides. In addition, we collected information on possible products of the remaining reagents not involved in the CPs.

2. Results and Discussion

2.1. Synthesis and Crystal Structures

For the synthesis of novel luminescent coordination polymers, the interaction of organic units, the linkers, and the metal cations as connectivity centers are significant in order to achieve an efficient emitter for a specific emission energy and thereby luminescence colour.[1] For lanthanide(III)-based compounds, it is essential to overcome the intrinsically low light uptake, which is a specific result of the parity forbidden character of all relevant intra-4f-transitions.

In order to achieve such a luminescent CP with wide options for the deliberate setting of the luminescence chromaticity, we chose the bis-salicylatoborate anion as linker, as it provides excited triplet states in a range of 29,000 to 27,500 cm^{-1}, suitable to sensitize Eu^{3+} and Tb^{3+} ions via an energy transfer to their excited 4f-states. As the anion, in principle, can feed the excited states of both Ln-ions, it is also suitable for a concept of multiple chromophores to achieve a luminescence chromaticity beyond the typical emission colours of the respective Ln-ions, which are green and red. Especially, a tuning of the chromaticity can be achieved by variation of the ratio of both emitters. This concept is based on the generation of one homogenous phase that contains both cations and the respective anion.

We selected the ionic liquid (IL) [EMIm][BSB], which provides both, the desired anion and a liquid phase for the synthesis that is consumed during the ionothermal reaction. Regarding the lanthanides, anhydrous chlorides $EuCl_3$ and $TbCl_3$ were selected. As the consumption of the liquid phase, namely the IL, brings the reaction to a halt, minor amounts of py were added, as stated previously.[16] Reactions at 180 °C performed in sealed ampoules gave products of the constitution $^1_\infty[Eu_xTb_{1-x}(BSB)_3(py)_2]$ as crystalline materials. So, in principle, the IL is transformed into a coordination polymer during the reaction. However, as not all parts of the reagents are included in the products, it was already a question before, what the remaining components do in the ionothermal reaction. Thus, in a first attempt, the sodium salt Na[BSB] was added in order to improve the yield via an increased $[BSB]^-$ concentration. NaCl is formed as byproduct as stated, previously.[16] A more detailed description of the ionothermal reaction can be found in Ref. [16]. In a second attempt, a control reaction was performed with yttrium chloride. In this case, we now successfully crystallized a phase of the remaining components $[EMIm]^+$ and Cl^- together with Y^{3+}: $[EMIm]_2[YCl_5(py)]$, which gives a possible answer to the question about the remaining components. The phase shows a higher solubility than the coordination polymers and it was formed as single crystals in addition to a microcrystalline powder of $^1_\infty[Y(BSB)_3(py)_2]$. Accordingly, in the ionothermal reaction, only the $[BSB]^-$ anion and a certain part of the Ln^{3+} amount are forming the coordination polymers, whereas $[EMIm]^+$, Cl^-, and the remaining Ln-content can form salt like byproducts soluble under the reaction conditions.

$^1_\infty[Eu_xTb_{1-x}(BSB)_3(py)_2]$ crystallizes in the monoclinic crystal system in the space group $P2_1/n$. The crystal structure is constituted by single strands of BSB-linked lanthanide ions, which are coordinated by the oxygen atoms of the anion and two equivalents of N atoms of py in a distorted dodecahedral coordination polyhedron (see Figure 1). The spiroborate anions show the tetrahedral oxygen coordination typical for borates.

As the crystal structure has already been described,[16] details can be retrieved from the respective reference. Also, this study did not head for the synthesis of large single crystals but for a suitable homogenous mixture of the two Ln-emitters Eu^{3+} and Tb^{3+} by a statistic replacement of both cations in the crystal structure. Due to the close relation of the ions and the reagents $EuCl_3$ and $TbCl_3$ regarding ionic radii and chemical character, mixing proved possible throughout a wide range for x = 0.75, 0.50, 0.25, without the formation of additional phases

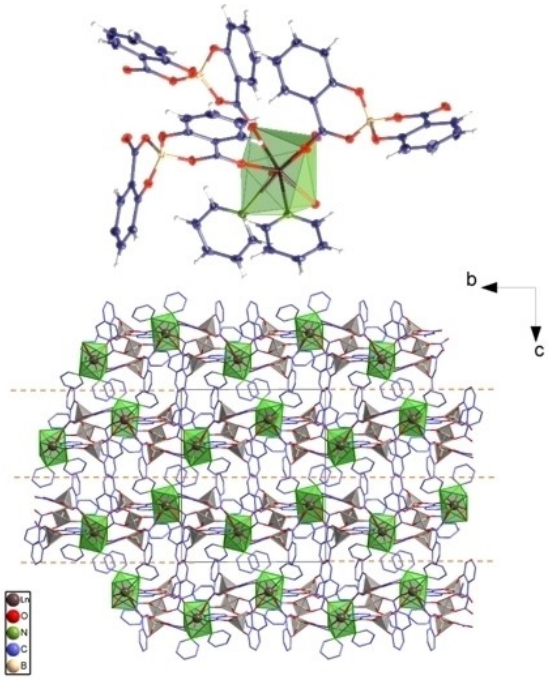


Figure 1. The coordination sphere (top) and crystal structure of $^1_\infty[Eu_xTb_{1-x}(BSB)_3(py)_2]$ as view along [−100] (bottom). Coordination polyhedra of the Ln-ions are marked in green, of boron in grey. H atoms have been omitted for clarity. Dotted orange lines shall indicate that the strands run along the b-axis.

© 2021 The Authors. Published by Wiley-VCH GmbH

(see Figure 2 for the results of X-ray powder diffraction). The PXRD patterns show all main reflections of the structure type $^{1}_{\infty}[Ln(BSB)_3(py)_2]$. No additional reflections are observed (except for reaction with additional Na[BSB], in which reflections of NaCl are observed in the bulk products. Previously, the strand like CP type $^{1}_{\infty}[Ln(BSB)_3(py)_2]$ (Ln=Y, La–Nd, Sm) was not observed for europium, terbium and the following lanthanides, but only the network type $^{2}_{\infty}[Ln(BSB)_3(py)]$ (Ln=Sm, Eu, Tb, Dy, Er).[16] For x=0.15 or 0.85, already phase mixtures of 1D- and 2D-CPs are observed. However, we can now show that both, the 1D- and the 2D-CP can be formed for more lanthanide ions and are not just separating the first and the second half of the lanthanide series.

In addition, by crystallization of $[EMIm]_2[YCl_5(py)]$ as single crystals, a new phase was detected that contains the components of the ionothermal reaction not present in the CP. The crystal structure shows that the compound is salt like, constituted by $[EMIm]^+$ cations and $[YCl_5(py)]^{2-}$ anions. The compound crystallizes in the orthorhombic crystal system in the space group *Pbcn*. The coordination of the Y atoms is constituted by five chlorine atoms and one py molecule. The Y–Cl distances are 260.1(2)–262.5(2) pm, and Y–N is 249.0(7) pm. The interatomic distances match with related phases, such as $[YCl_3(py)_4]$,[17] $[YCl_2(Ph_3PO)_4]Cl\cdot 2.5EtOH\cdot H_2O$,[18] and $[(Me_2NCH_2CH_2)C_2B_9H_{10}]YCl(thf)_2$.[19] The structure is related to complexes such as $[HPy]_2[LnCl_5(py)]$,[20] which contains pyridinium cations for charge compensation. Both exhibit Cl–H-hydrogen bonding, the closest in $[EMIm]_2[YCl_5(py)]$ being 263.9(8) pm (see Figure 3).

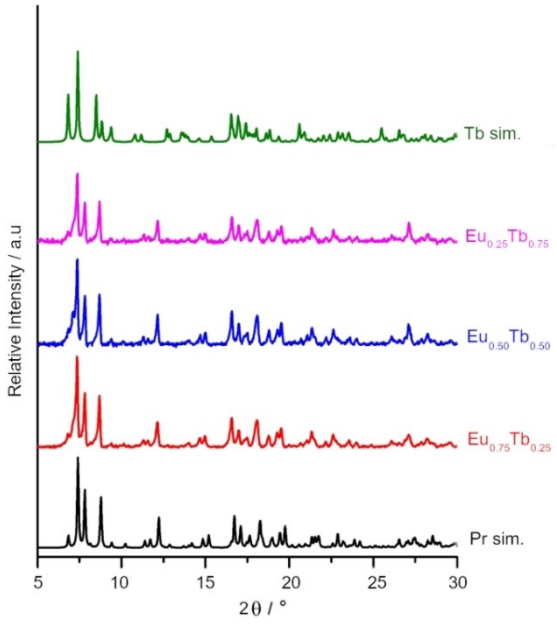


Figure 2. Comparison of X-ray powder patterns: powder pattern of $^{2}_{\infty}[Tb(BSB)_3(py)]$ simulated from single crystal data (top, green); recorded patterns of $^{1}_{\infty}[Eu_xTb_{1-x}(BSB)_3(py)_2]$ (centre, magenta, blue and red, representing three different Ln-ratios) and a pattern of $^{1}_{\infty}[Pr(BSB)_3(py)_2]$, also simulated from X-ray single crystal data (bottom, black).

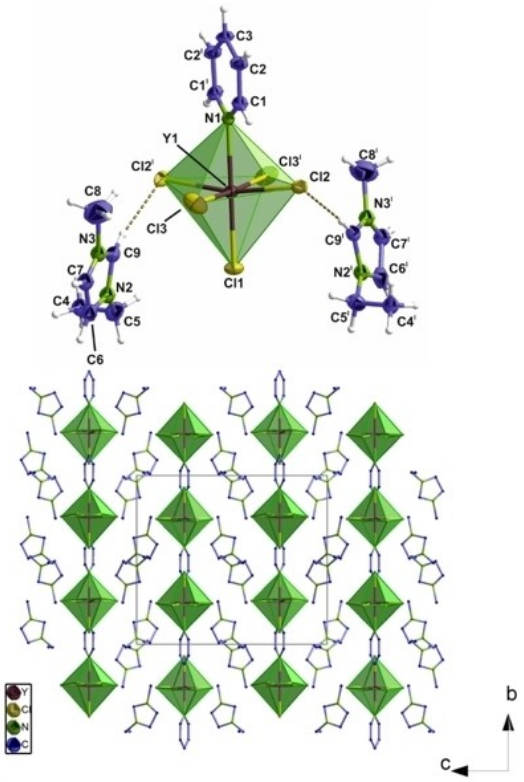


Figure 3. Coordination sphere of the Y^{3+} ions in $[EMIm]_2[YCl_5(py)]$ and H-bonding to $[EMIm]^+$ cations (top); the crystal structure of $[EMIm]_2[YCl_5(py)]$ as view along [−100] (bottom). Coordination polyhedra of the yttrium ions are marked in green, of boron in grey. H atoms have been omitted for clarity.

2.2. Photoluminescence and Vibrational Spectroscopy

Excitation and emission spectra of the one-dimensional CPs $^{1}_{\infty}[Eu_xTb_{1-x}(BSB)_3(py)_2]$ and of $[EMIm]_2[YCl_5(py)]$ were recorded and are depicted in Figure 4 and 5.

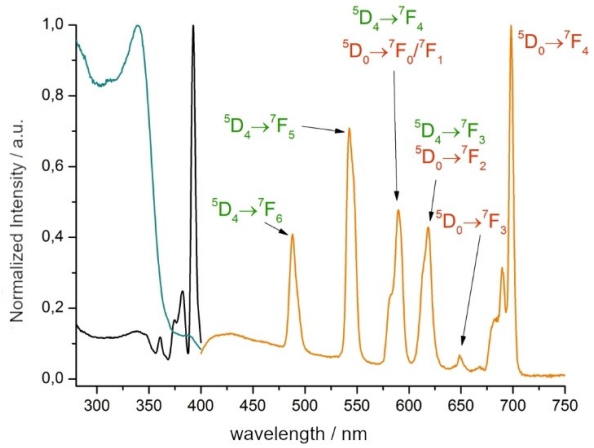


Figure 4. Excitation and emission spectra of $^{1}_{\infty}[Eu_xTb_{1-x}(BSB)_3(py)_2]$, for x=0.75 (turquoise: $\lambda_{em}=543$ nm, black: $\lambda_{em}=698$ nm, orange: $\lambda_{exc}=340$ nm) and an identification of the 4f-transitions of Tb^{3+} (green) and Eu^{3+} (red).

© 2021 The Authors. Published by Wiley-VCH GmbH

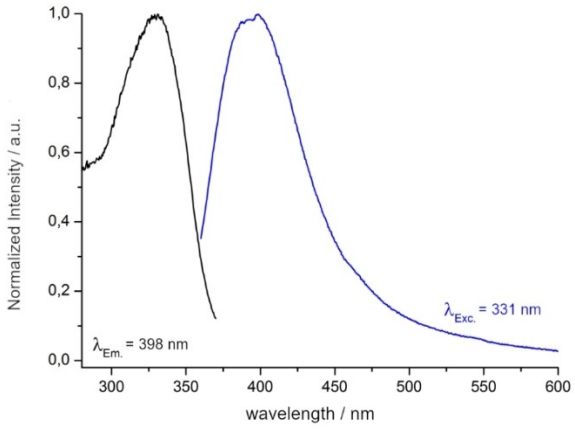


Figure 5. Excitation (black) and emission spectrum (blue) of $[EMIm]_2[YCl_5(py)]$.

Excitation of $^1_\infty[Eu_xTb_{1-x}(BSB)_3(py)_2]$ is based on two processes, depending on the metal ratio: For x = 0.25–0.5, ligand-based processes dominate. Here, $^*S_1 \leftarrow S_0$ transitions of $[BSB]^-$ dominate the processes, which can be seen in comparison to Na[BSB] ($\lambda_{max} = 340$ nm, see Figure S1, Supporting Information). The latter is useful for comparison, as it is free of any pyridine that can also be part of the PL processes. Typically, pyridine and its derivatives exhibit $^*S_1 \leftarrow S_0$ and $^*\pi \leftarrow \pi$ transitions in the region of 260–300 nm.[21] For x > 0.5, also direct 4f-excitation of Eu^{3+} is observed ($\lambda_{max.} = 394$ nm), depending on the emission wavelength, the excitation is determined for. Here a distinct difference between resulting Tb^{3+} and Eu^{3+}-based emission can be observed: For $\lambda_{em} = 543$ nm, the maximum of Tb^{3+} emission, the ligand-based excitation dominates, indicating a good energy transfer to the terbium ions. In contrast, direct europium excitation is also evident for $\lambda_{em} = 698$ nm, the maximum of Eu^{3+} emission, indicating a less efficient energy transfer from excited ligand states to the Eu^{3+} ions.

The emission spectra of $^1_\infty[Eu_xTb_{1-x}(BSB)_3(py)_2]$ show a broad band ligand-based emission from 400 to 575 nm, probably of triplet states of the $[BSB]^-$ anion. The typical $[BSB]^-$ fluorescence < 400 nm is not observed, so that the region was subsequently cut off by an edge filter in order to fully collect the range of Ln^{3+} emission. As depicted in Figure 4, the CPs exhibit 4f-based emission of both lanthanide ions. For Tb^{3+}, transitions $^5D_4 \rightarrow {}^7F_J$, J = 6–3, can be identified, and for Eu^{3+}, transitions $^5D_0 \rightarrow {}^7F_J$, J = 0–4, are observed.[15,22] Remarkably, and in contrast to $^2_\infty[Eu(BSB)_3(py)]$,[16b] the most intense transition of Eu^{3+} is $^5D_0 \rightarrow {}^7F_4$ ($\lambda_{max} = 698$ nm) and not $^5D_0 \rightarrow {}^7F_2$ ($\lambda_{em} = 615$ nm). As the components of both CPs are identical, the chemical and binding interaction, polarizability and covalence are supposed also to be quite similar. Accordingly, we consider the symmetry of the distorted dodecahedral coordination sphere in $^1_\infty[Eu_xTb_{1-x}(BSB)_3(py)_2]$ to be responsible for this difference. As expected, the Tb^{3+} based emission follows the usual course, with the transition $^5D_4 \rightarrow {}^7F_5$ being the highest in intensity (see also Figures S2 and S3 for more details and spectra for x = 0.25 and x = 0.5).

Altogether, the combination of Tb^{3+} and Eu^{3+}-based emission lines results in a tunability of the emission chromaticity.

Typically, Tb^{3+} results in green and Eu^{3+} in red emission. The mixed CPs $^1_\infty[Eu_xTb_{1-x}(BSB)_3(py)_2]$, x = 0.25–0.75, result in overall chromaticities in-between. This includes the yellow region, known as the yellow gap of primary LED phosphors.[23] Figure 6 displays a chromaticity diagram according to CIE[24] that identifies the colour coordinates of the mixed CPs and of the border phases $^2_\infty[Ln(BSB)_3(py)]$, Ln = Eu, Tb.[16b]

Although the red emission in $^1_\infty[Eu_xTb_{1-x}(BSB)_3(py)_2]$ shows the transition $^5D_0 \rightarrow {}^7F_4$ as most intense for Eu^{3+}, which is bathochromically shifted to $^5D_0 \rightarrow {}^7F_2$, viz, actually being even more red in nature, even for 0.75 europium equivalents, the chromaticity is closer to the white point than to red. Also, a potential metal-to-metal energy transfer, which should usually transfer energy $Tb^{3+} \rightarrow Eu^{3+}$ as a downshift does not seem to significantly feed the europium-based emission. Instead, Tb^{3+}-based transitions dominate in intensity. As described for the excitation spectra, the better energetic match between excited ligand states and the excited 4f-states of Tb^{3+} compared to the excited 4f states of Eu^{3+}, which are lower in energy, is held responsible for the domination of terbium-based emission. Accordingly, the course of x,y colour coordinates in the chromaticity diagram is not linear, which is also partly observed for $[Tb_{2x}Eu_{2-2x}(bdc)_3(H_2O)_4]_\infty$, bdc^{2-} = benzene-dicarboxylate.[25] This is different to the linear chromaticity change shown for $^2_\infty[Gd_{2-x-y}Eu_xTb_yCl_6(bipy)_3] \cdot 2bipy$, bipy = 4,4′-bipyridine,[26] or $[Ln_4(btec)_3(H_2O)_{12} \cdot 20H_2O]_\infty$, $btec^{4-}$ = benzene-tetracarboxylate.[27] This consideration is also corroborated by quantum yield determinations of $^1_\infty[Eu_xTb_{1-x}(BSB)_3(py)_2]$ that

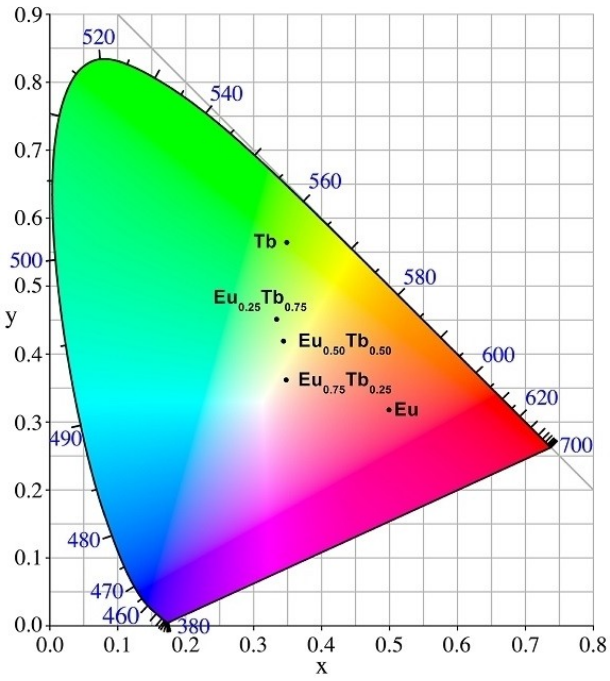


Figure 6. Chromaticity diagram according to CIE and colour coordinates x,y of the compounds $^1_\infty[Eu_xTb_{1-x}(BSB)_3(py)_2]$ for respective x as well as for the pure Eu- and Tb-phases $^2_\infty[Ln(BSB)_3(py)]$.

© 2021 The Authors. Published by Wiley-VCH GmbH

are highest for the most terbium rich sample with x = 0.25, and decrease from QY = 0.59 to QY = 0.16 for x = 0.75, indicating a better energy transfer from the ligand to Tb^{3+} than to Eu^{3+}, resulting in a more efficient emission for a higher Tb-content.

In addition, the photoluminescence properties of $[EMIm]_2[YCl_5(py)]$ were investigated (see Figure 5). As Y^{3+} cannot take part in or offer metal-based transitions according to its configuration, the compound is luminescent with broad banded processes for both, excitation and emission. Therefore, it is also a suitable example to illuminate a possible participation of pyridine, which is present in the luminescent products presented. However, both product maxima in excitation and emission are outside the range and lower in energy than for py derivatives (260–300 nm).[21] It can be estimated that the high energetic shoulder in the excitation spectrum may result also from py-based excitation. However, this is already close to the spectral range of the PL spectrometer. From the literature, the $[EMIm]^+$ cation is known to show excitation $^*S_1 \leftarrow S_0$ for >300 nm and fluorescence in emission that can be bathochromically shifted from IL to low melting salts depending on the excitation wavelength.[28] Accordingly, we mainly assign the photoluminescence properties of $[EMIm]_2[YCl_5(py)]$ to the cations of the original IL and not to py. The overall PL intensity is low, compared to $^1{}_\infty[Eu_xTb_{1-x}(BSB)_3(py)_2]$.

Also, vibrational spectra of the compounds were recorded. The respective bands are given in detail in the experimental section. Characteristic vibrations of $^1{}_\infty[Eu_xTb_{1-x}(BSB)_3(py)_2]$ are bands of the C=O units of the bis-salicylatoborate anion $\tilde{\nu}$ ($\tilde{\nu}$ = 1600 cm^{-1}) and the B–O stretching mode ($\tilde{\nu}$ = 750 cm^{-1}). Actually, IR-spectroscopy indicated that $[EMIm]_2[YCl_5(py)]$ is highly hygroscopic and takes up water quickly. The IR-spectrum shows a dominant broad band up to 3600 cm^{-1} for the OH vibration that overlaps with C–H vibrations of the $[EMIm]^+$ cation ($\tilde{\nu}$ = 2900–3000 cm^{-1}). Furthermore, stretching modes of the C=C bond and valence modes of the aromatic ring system are evident at $\tilde{\nu}$ = 1632 and 1442, 1486 cm^{-1}, respectively (for IR spectra, see Figures S4 and S5 in the SI).

3. Conclusions

Luminescence chromaticity tuning between green, yellow and red was achieved by statistic replacement of Eu^{3+} and Tb^{3+} in the CPs $^1{}_\infty[Eu_xTb_{1-x}(BSB)_3(py)_2]$, containing the bis-salicylatoborate anion. Ionothermal reactions of [EMIm][BSB] together with lanthanide trichlorides were carried out with slight additions of pyridine. In the respective reactions, CPs are formed by direct conversion of an IL utilizing its anions as linkers. In addition to the CPs, the remaining reagents form salts of the type $[EMIm]_2[LnCl_5(py)]$, as proven for single crystals containing Y^{3+}, which helps clarifying the overall ionothermal reaction for the parts of the reagents that do not constitute the coordination polymers. Instead, they can crystallize as salts. The luminescence of $^1{}_\infty[Eu_xTb_{1-x}(BSB)_3(py)_2]$ is based on a sensitizer effect of the $[BSB]^-$ anion followed by emission through intra-4f transitions of trivalent europium and terbium. The chromaticity is additive, being determined by the ratio of both Ln-ions in the solid solutions.

Experimental Section

All manipulations were performed under inert conditions (Ar atmosphere) using vacuum line, glovebox (MBraun, Labmaster SP and Innovative Technology, PureLab), Schlenk and Duran® glass ampoule techniques. $LnCl_3$, Ln=Eu, Tb, Y, (Strem Chemicals, 99.9%) and anhydrous pyridine (Alfa Aesar, 99.5%) were used as purchased. Na[BSB] and [EMIm][BSB] were synthesized according to literature known procedures.[29]

Synthesis of $^1{}_\infty[Eu_xTb_{1-x}(BSB)_3(py)_2]$

For the formation of the coordination polymers, mixtures of $EuCl_3$ and $TbCl_3$ (0.2 mmol, 52–54 mg, see Supporting Information, Tab. S1 for further details) [EMIm][BSB] (0.45 mmol, 178 mg), optional Na[BSB] (0.30 mmol, 72 mg), and pyridine (C_5H_5N, 0.1 mL) were sealed in an evacuated Duran® glass ampoule. The ampoule was heated to 180 °C in 6 h. The temperature was held for 96 h. Then the reaction mixture was cooled to room temperature at a rate of 1 °C/h. A colourless crystalline product formed. Subsequently, the excess liquid was removed, the products were washed three times with pyridine (0.3 mL), and dried under vacuum ($p < 10^{-2}$ mbar) for 5 h. Na[BSB] resulted in an increased yield by 10–15%. However, pure products are only possible without the addition of Na[BSB], as the resulting NaCl also precipitates. The following analytical data are given for the pure, crystalline products:

$^1{}_\infty[Eu_{0.75}Tb_{0.25}(BSB)_3(py)_2]$: yield: 65 mg = 28%. MIR (ATR): $\tilde{\nu}$ = (2960 w, 1692 m, 1658 m, 1599 s, 1469 s, 1350 m, 1272 m, 1244 m, 1145 m, 1092 m, 1037 m, 1006 m, 959 m, 753 s) cm^{-1}. Elemental analysis of $C_{52}H_{34}B_3N_2O_{18}Eu_{0.75}Tb_{0.25}$ (M = 1160.97 g mol^{-1}): calcd.: C 53.80; H 2.95; N 2.41%; found: C 53.52; H 3.26; N 2.34%.

$^1{}_\infty[Eu_{0.50}Tb_{0.50}(BSB)_3(py)_2]$: yield: 59 mg = 25%. MIR (ATR): $\tilde{\nu}$ = (2965 w, m, 1690 w, 1658 m, 1601 s, 1469 s, 1356 m, 1272 s, 1244 m, 1144 m, 1092 m, 1037 m, 1005 m, 985 m, 960 m, 753 s) cm^{-1}. Elemental analysis of $C_{52}H_{34}B_3N_2O_{18}Eu_{0.50}Tb_{0.50}$ (M = 1162.70 g mol^{-1}): calcd.: C 53.72; H 2.95; N 2.41%; found: C 54.78; H 3.31; N 2.40%.

$^1{}_\infty[Eu_{0.25}Tb_{0.75}(BSB)_3(py)_2]$: yield: 62 mg = 27%. MIR (ATR): $\tilde{\nu}$ = (2965 w, 1691 m, 1600 s, 1468 s, 1355 m, 1244 m, 1133 m, 1091 m, 1033 m, 1008 m, 959 m, 752 s) cm^{-1}. Elemental analysis of $C_{52}H_{34}B_3N_2O_{18}Eu_{0.25}Tb_{0.75}$ (M = 1164.45 g mol^{-1}): calcd.: C 53.95; H 2.96; N 2.42%; found: C 54.28; H 3.55; N 2.65%.

Synthesis of $[EMIm]_2[YCl_5(py)]$

YCl_3 (0.15 mmol, 29.3 mg) was mixed with [EMIm][BSB] (0.45 mmol, 177.4 mg), and the reagents were sealed in an evacuated Duran® glass ampoule together with pyridine (2.5 mmol, 0.20 mL). The ampoule was heated to 160 °C at a rate of 30 °C/h. The temperature was held for 96 h. The reaction mixture was then cooled to room temperature at a rate of 4 °C/h. A colourless crystalline product formed which proved to be $^1{}_\infty[Y(BSB)_3(py)_2]$. In addition, colourless single crystals of $[EMIm]_2[YCl_5(py)]$ were formed that were distinguishable by differences in the crystal shape. The excess liquid was removed, and the products were washed two times with pyridine (0.5 mL), and dried under vacuum ($p < 10^{-2}$ mbar). The solid products were separated manually by Pasteur methods. Yield 33 mg = 39%. MIR (ATR): $\tilde{\nu}$ = (3148 w, 3098 w, 3063 m, 1632 m, 1602 w, 1573 w, 1486 m, 1442 m, 1171 s, 762 m) cm^{-1}. Elemental

© 2021 The Authors. Published by Wiley-VCH GmbH

analysis of $C_{17}H_{27}Cl_5N_5Y$ ($M = 567.59\ g\,mol^{-1}$): calcd.: C 35.97; H 4.79; N 12.34%; found: C 38.53; H 5.44; N 12.35%.

Single-Crystal X-Ray Diffraction

A suitable single crystal of $[EMIm]_2[YCl_5(py)]$ was selected from the crystalline bulk product and treated with high-viscosity perfluorinated ether (99.9%, abcr). Data collection was performed with a Bruker AXS Apex II diffractometer with a Helios mirror at 100 K utilizing the Bruker AXS software package.[30] Data processing was accomplished with the XPREP package.[31] The crystal structure was solved by direct methods using SHELXT,[32] and the structure refinement was carried out by least-squares techniques with SHELXL[32] on the graphical platform OLEX2.[33] Hydrogen atoms were calculated using geometric constraints, whereas all non-hydrogen atoms were refined anisotropically by least-square techniques. The supporting Information contains the crystallographic data and selected interatomic distances and angles. The crystallographic data was also deposited at the Cambridge Crystallographic Data Centre and can be obtained free of charge quoting the CCDC number 1586260.

Powder X-Ray Diffraction

Samples (5–10 mg) for powder X-ray diffraction were ground in a mortar and transferred to Lindemann glass capillaries ($\varnothing = 0.5$ mm). Diffraction data was obtained in transmission geometry with a Bruker AXS D8 Discover Da Vinci powder X-ray diffractometer provided with a Lynxx-Eye detector. X-Ray radiation (Cu-$K_{\alpha 1}$; $\lambda =$ 154.06 pm) was focused with a Goebel mirror and the measured diffraction patterns were analysed with the Bruker AXS Diffrac software suite.

Elemental Analysis

Elemental analysis for C, H, and N was conducted on a Vario EL instrument (Elementar Analysensysteme GmbH).

Photoluminescence Spectroscopy

Excitation and emission spectra were recorded with a Horiba Jobin Yvon Spex Fluorolog 3 spectrometer equipped with a 450 W Xe lamp, double-grated excitation and emission monochromators and a photomultiplier tube (R928P) using the FluorEssence software. Both, excitation and emission spectra were corrected for the spectral response of the monochromators and the detector by application of the correction spectra provided by the manufacturer. Furthermore, excitation spectra were corrected for the spectral distribution of the lamp intensity by use of a photodiode reference detector. In addition, an edge filter (GG400, Newport) was used for emission spectra of $^1{}_\infty[Eu_{0.75}Tb_{0.25}(BSB)_3(py)_2]$ after the respective area below 400 nm was checked to be without emission intensity in order to allow for recording of the full Eu^{3+} emission range. Photoluminescence quantum yields were determined with the above-mentioned HORIBA Jobin Yvon Spex Fluorolog 3 spectrometer equipped with a HORIBA Quanta-φ F-3029 Integrating Sphere using a FluoroEssence™ software. For the measurements, solid samples were filled into Starna Micro Cell cuvettes 18-F/ST/C/Q/10 (fluorescence with ST/C closed-cap, material UV quartz glass Spectrosil Q, pathlength 10 mm, matched). Dry barium sulphate was used as a reference material. Each sample was measured at least three times to generate an average; the range of trustworthiness is 10% of the value.

Acknowledgements

The authors are grateful for financial support from the Deutsche Forschungsgemeinschaft (DFG) within the priority program SPP1708 and the projects MU-1562/8-2 and FI-1628/4-2. Furthermore, Sven H. Zottnick thanks the Evangelisches Studienwerk Villigst e. V. for a PhD scholarship.

Conflict of Interest

The authors declare no conflict of interest.

Keywords: borates · coordination polymers · ionic liquids · lanthanides · luminescence

[1] a) M. D. Allendorf, C. A. Bauer, R. K. Bhakta, R. J. T. Houk, *Chem. Soc. Rev.* **2009**, *38*, 1330–1352; b) J. Rocha, L. D. Carlos, F. A. A. Paz, D. Ananias, *Chem. Soc. Rev.* **2011**, *40*, 926–940; c) Y. Cui, Y. Yue, G. Qian, B. Chen, *Chem. Rev.* **2012**, *112*, 1126–1162; d) J. Heine, K. Müller-Buschbaum, *Chem. Soc. Rev.* **2013**, *42*, 9232–9242; e) S. Roy, A. Chakraborty, T. K. Maji, *Coord. Chem. Rev.* **2014**, *273*, 139–164; f) Z. Hu, B. J. Deibert, J. Li, *Chem. Soc. Rev.* **2014**, *43*, 5815–5840; g) K. Müller-Buschbaum, F. Beuerle, C. Feldmann, *Microporous Mesoporous Mater.* **2015**, *216*, 171–199; h) F. Saraci, V. Quezada-Novoa, P. R. Donnarumma, A. J. Howarth, *Chem. Soc. Rev.* **2020**, *49*, 7949—7977. 10.1039/D0CS00292E.

[2] a) Y. Du, H. Yang, J. M. Whiteley, S. Wan, Y. Jin, S. H. Lee, W. Zhang, *Angew. Chem. Int. Ed.* **2016**, *55*, 1737–1741; b) H. Danjo, T. Nakagawa, K. Katagiri, M. Kawahata, S. Yoshigai, T. Miyazawa, K. Yamaguchi, *Cryst. Growth Des.* **2015**, *15*, 384–389; c) R. Nishiyabu, Y. Kubo, T. D. James, J. S. Fossey, *Chem. Commun.* **2011**, *47*, 1124–1150; d) H. Hartmann, *J. Prakt. Chem.* **1986**, *328*, 755–762.

[3] a) P. Bag, M. E. Itkis, D. Stekovic, S. K. Pal, F. S. Tham, R. C. Haddon, *J. Am. Chem. Soc.* **2015**, *137*, 10000–10008; b) S. K. Pal, P. Bag, M. E. Itkis, F. S. Tham, R. C. Haddon, *J. Am. Chem. Soc.* **2014**, *136*, 14738–14741.

[4] a) K. Xu, *Chem. Rev.* **2014**, *114*, 11503–11618; b) K. Xu, *Chem. Rev.* **2004**, *104*, 4303–4417.

[5] a) A. Swiderska-Mocek, D. Naparstek, *Electrochim. Acta* **2016**, *204*, 69–77; b) O. M. Korsun, O. N. Kalugin, I. O. Fritsky, O. V. Prezhdo, *J. Phys. Chem. C* **2016**, *120*, 16545–16552; c) H. Xiang, P. Shi, P. Bhattacharya, X. Chen, M. Dei, M. E. Bowden, J. Zheng, J.-G. Zhang, W. Xu, *J. Power Sources* **2016**, *318*, 170–177.

[6] a) M. Kunze, S. Passerini, A. Lex-Balducci, S. Nowak, R. W. Schmitz, M. Winter, WO 2012/069554, **2012**; b) Z.-M. Xue, J.-F. Zhao, J. Ding, C.-H. Chen, *J. Power Sources* **2010**, *195*, 853–856; c) Z.-M. Xue, J. Ding, W. Zhou, C.-H. Chen, *Electrochim. Acta* **2010**, *55*, 3838–3844; d) Z.-M. Xue, W. Zhou, J. Ding, C.-H. Chen, *Electrochim. Acta* **2010**, *55*, 5342–5348.

[7] a) S. Kaymaksiz, F. Wilhelm, M. Wachtler, M. Wohlfahrt-Mehrens, C. Hartnig, I. Tschernych, U. Wietelmann, *J. Power Sources* **2013**, *239*, 659–669; b) A. Downard, M. Nieuwenhuyzen, K. R. Seddon, J.-A. van den Berg, M. A. Schmidt, J. F. S. Vaughan, U. Welz-Biermann, *Cryst. Growth Des.* **2002**, *2*, 111–119; c) Z.-M. Xue, K.-N. Wu, B. Liu, C.-H. Chen, *J. Power Sources* **2007**, *171*, 944–947; d) Z. Huang, S. Wang, R. D. Dewhurst, N. V. Ignat'ev, M. Finze, H. Braunschweig, *Angew. Chem.* **2020**, *132*, 8882–8900; *Angew. Chem. Int. Ed.* **2020**, *59*, 8800–8816.

[8] a) W. Xu, L.-M. Wang, R. A. Nieman, C. A. Angell, *J. Phys. Chem. B* **2003**, *107*, 11749–11756; b) M. Yang, J. N. Zhao, Q. S. Liu, L. X. Sun, P. F. Yan, Z. C. Tan, U. Welz-Biermann, *Phys. Chem. Chem. Phys.* **2011**, *13*, 199–206.

[9] a) P. Y. Zavalij, S. Yang, M. S. Whittingham, *Acta Crystallogr. Sect. B* **2004**, *60*, 716–724; b) P. Y. Zavalij, S. Yang, M. S. Whittingham, *Acta Crystallogr. Sect. B* **2003**, *59*, 753–759; c) J. Bassett, P. J. Matthews, *J. Inorg. Nucl. Chem.* **1978**, *40*, 987–992.

[10] S. H. Zottnick, J. R. Sorg, J. A. P. Sprenger, M. Finze, K. Müller-Buschbaum, *Z. Anorg. Allg. Chem.* **2017**, *643*, 53–59.

[11] K. D. Matthews, I. A. Kahwa, M. P. Johnson, J. T. Mague, G. L. McPherson, *Inorg. Chem.* **1993**, *32*, 1442–1444.

[12] A. S. Gajadhar-Plummer, I. A. Kahwa, A. J. P. White, D. J. Williams, *Inorg. Chem.* **1999**, *38*, 1745–1753.

© 2021 The Authors. Published by Wiley-VCH GmbH

[13] R. K. Das, E. Barnea, T. Andrea, M. Kapon, N. Fridman, M. Botoshansky, M. S. Eisen, *Organometallics* **2015**, *34*, 742–752.
[14] S. H. Zottnick, J. A. P. Sprenger, M. Finze, K. Müller-Buschbaum, *Z. Anorg. Allg. Chem.* **2018**, *644*, 1445–1450.
[15] a) J.-C. G. Bünzli, C. Piguet, *Chem. Soc. Rev.* **2005**, *34*, 1048–1077; b) K. Binnemans, *Chem. Rev.* **2009**, *109*, 4283–4374; c) S. V. Eliseeva, J.-C. G. Bünzli, *Chem. Soc. Rev.* **2010**, *39*, 189–227; d) L. V. Meyer, F. Schönfeld, K. Müller-Buschbaum, *Chem. Commun.* **2014**, *50*, 8093–8108.
[16] a) S. H. Zottnick, J. R. Sorg, J. A. P. Sprenger, M. Finze, K. Müller-Buschbaum, *Z. Anorg. Allg. Chem.* **2015**, *641*, 164–167; b) S. H. Zottnick, J. A. P. Sprenger, M. Finze, K. Müller-Buschbaum, *Eur. J. Inorg. Chem.* **2017**, 1355–1363.
[17] J.-S. Li, B. Neumüller, K. Dehnicke, *Z. Anorg. Allg. Chem.* **2002**, *628*, 45–50.
[18] N. J. Hill, W. Levason, M. C. Popham, G. Reid, M. Webster, *Polyhedron* **2002**, *21*, 445–455.
[19] M.-S. Cheung, H.-S. Chan, Z. Xie, *Organometallics* **2005**, *24*, 4207–4215.
[20] J.-S. Li, B. Neumüller, K. Dehnicke, *Z. Anorg. Allg. Chem.* **2002**, *628*, 2785–2789.
[21] a) I. Yamazaki, H. Baba, *J. Chem. Phys.* **1977**, *66*, 5826–5827; b) T. Handa, Y. Utena, H. Yajima, T. Ishii, H. Morita, *J. Phys. Chem.* **1986**, *90*, 2589–2596; c) L. Pellegatti, J. Zhang, B. Drahos, S. Villette, F. Suzenet, G. Guillaumet, S. Petoud, E. Toth, *Chem. Commun.* **2008**, 6591–6593.
[22] a) G. Blasse, A. Bril, *Appl. Phys. Lett.* **1967**, *11*, 53–55; b) P. Dorenbos, *J. Lumin.* **2000**, *91*, 91–106; c) S. H. Zottnick, J. R. Sorg, K. Müller-Buschbaum, C. Fouassier, Luminescence in *Encyclopedia of Inorganic and Bioinorganic Chemistry, Vol. 2* (Eds.: R. A. Scott), Wiley VCH, Chichester, **2019**.
[23] a) S. Nakamura, T. Mukai, M. Senoh, *Jpn. J. Appl. Phys.* **1992**, *31*, 1258–1266; b) E. F. Schubert, *Light-emitting diodes*, II. Edition, Cambridge University Press, Cambridge, New York, **2006**.
[24] a) T. Smith, J. Guild, *Trans. Opt. Soc.* **1931**, *33*, 73–134; b) B. Becerir, *J. Text. Eng. Fashion Technol.* **2017**, *1*, 240–244.
[25] V. Haquin, M. Etienne, C. Daiguebonne, S. Freslon, G. Calvez, K. Bernot, L. Le Pollès, S. E. Ashbrook, M. R. Mitchell, J.-C. Bünzli, S. V. Eliseeva, O. Guillou, *Eur. J. Inorg. Chem.* **2013**, 3464–3476.
[26] P. R. Matthes, C. J. Höller, M. Mai, J. Heck, S. J. Sedlmaier, S. Schmiechen, C. Feldmann, W. Schnick, K. Müller-Buschbaum, *J. Mater. Chem.* **2012**, *22*, 10179–10187.
[27] S. Freslon, Y. Luo, C. Daiguebonne, G. Calvez, K. Bernot, O. Guillou, *Inorg. Chem.* **2016**, 55, 794–802.
[28] a) A. Paul, P. K. Mandal, A. Samanta, *J. Phys. Chem. B* **2005**, *109*, 9148–9153; b) A. Paul, P. K. Mandal, A. Samanta, *Chem. Phys. Lett.* **2005**, *402*, 375–379; c) I. Billard, G. Moutiers, A. Labet, A. El Azzi, C. Gaillard, C. Mariet, K. Lützenkirchen, *Inorg. Chem.* **2003**, *42*, 1726–1733.
[29] M. Bishop, S. G. Bott, A. R. Barron, *Dalton Trans.* **2000**, 3100–3105.
[30] Apex 2 Suite, Bruker AXS Inc., Madison, Wisonsin, WI, **2014**.
[31] G. M. Sheldrick, *Acta Crystallogr. Sect. A* **2008**, *64*, 112–122.
[32] G. M. Sheldrick, *Acta Crystallogr. Sect. A* **2015**, *71*, 3–8.
[33] O. V Dolomanov, L. J. Bourhis, R. J. Gildea, J. A. K. Howard, H. Puschmann, *J. Appl. Crystallogr.* **2009**, *42*, 339–341.

Manuscript received: August 31, 2020
Revised manuscript received: December 10, 2020

© 2021 The Authors. Published by Wiley-VCH GmbH